Adsorption Mechanisms: Synthetic Inorganic and Synthetic Organic Competition Onto Adsorbent

Roslan Omar[a,b], Ab Aziz Abdul Latiff[b], Raffidah Hamdan[b], Elias Ismail[a] Zailan Zahid[a] , Azlin Selamat[a] , Shazatul Irwan[a], Siddiq Mustafa[b]

[a]Water Academic Department, SAJ Holdings Sdn. Bhd, Jalan Garuda 80350 Johor Bahru, Malaysia

[b] Faculty of Civil Engineering and Environment, Univesity of Tun Hussein Onn Malaysia, Parit Raja, 86400 Batu Pahat, Johor, Malaysia

***Abstract*-- Mass transfer is necessary for separation and adsorption processes. Even though mass transfer resistance controls the kinetic adsorption rate, little is known about the adsorption of a solute on a porous material from surface water. This study investigates the adsorption competition of five different synthetic micropollutants and the influence of the substances' characteristics, such as molecular weight and density of mercury (Hg), cadmium (Cd), arsenic (As), dichlorodiphenyltrichloroethane (DDT), and chlordane (CHLs), on three different types of granular activated carbon using a column dynamic reactor. The application of modified mass transfer models allows us to determine the mass transfer resistance during the adsorption of more solutes on porous materials. Adsorption of synthetics Hg, Cd, As, DDT and CHLs onto SIG, SAG, and BAG that were started at difference percentage of outflow, although the sample was taken similarly, the outcomes were showed a significance competition between adsorbates onto adsorbents. Adsorption onto SIG showed the percentage outflow for Hg, Cd, As, DDT and CHLs (mixed solutions) were 20%, 19%, 19%, 16% and 8% respectively. Moreover, the adsorption onto SAG showed the percentage outflow were 16%, 13%, 19%, 23% and 24% respectively. The adsorption of Hg, Cd, As, DDT and CHLs (mixed solutions) onto BAG showed the percentage outflow were 16%, 8%, 5%, 18% and 8% respectively. The mass transfer resistance depends on the film mass transfer and porous diffusion before and after breakthrough. The results of this study advance our understanding of novel approaches for investigating the mass transfer resistance of the adsorption of solutes on porous materials from water.**

***Index Term*-- adsorption, mass transfer, micro pollutants, granular activated carbon, mathematical model**

1. INTRODUCTION

Empirical and theoretical models have been proposed for different applications to study the mechanisms of mass transfer from adsorption in a solution [1]. For example, a theoretical model describes the breakthrough curves for pesticide adsorption [2], and multi-component experimental data were modelled using extended Langmuir-based equations and the ideal adsorbed solution theory [3]. Therefore, proper equations should be proposed for determining the separation performance to increase the adsorption capacity. Particular equation designs are necessary for incorporating the presence of contaminants when designing industrial-scale columns [4].

Many developed models and theories are only valid for specific purposes [5, 6]. For example, the mass transfer factor models proposed by Fulazzaky [7] are valid for determining the mass transfer resistance for the adsorption of a single solute on granular activated carbon (GAC) from an aqueous solution. However, because surface water contains many different solutes, these models cannot describe the relatively complex competitive adsorption mechanisms of two or more solutes. The mechanisms of solute adsorption on porous materials from aqueous solutions can be represented by three successive steps: film mass transfer, porous diffusion, and fixation [8]. One advantage of mass transfer models is that they can provide an explicit framework for understanding further improvements in adsorption capacity, adsorbate-adsorbent affinity, and other properties that are necessary for realizing wide-ranging applications.

The objective of modelling is to develop mathematical tools that allow for the integration of knowledge regarding global, external, and internal mass transfer phenomena. The modified mass transfer factor models proposed in this study could be widely applied to determine the mass transfer resistance for the adsorption of one or more solutes on porous materials from surface water. The equations governing mass transfer processes are based on the principle of mass conservation [9, 10]. Many different situations can be classified as a mass transfer. Ideally, all of these situations can be modelled using the most general mass transfer equation [11]. When developing a correlation between models and theories [12], it is important to understand the models systematically. Because the process of fixing solutes on acceptor sites is quick [13], this mass transfer step does not impede solute transport. Therefore, the mass transfer resistance depends on the film mass transfer, porous diffusion, or both.

In this study, detailed systematic adsorption studies of mercury (Hg), cadmium (Cd), arsenic (As), dichlorodiphenyltrichloroethane (DDT), and chlordane (CHLs) from synthetic water samples were conducted. The primary objectives of this study are to (1) elucidate multi-solute adsorption, (2) investigate the influence of adsorbate characteristics such as molecular weight and density owing to the reaction between adsorbates in bulk samples, and (3)

investigate the competition of five synthetic micro pollutants during adsorption.

Nomenclature

a - surface of interfacial liquid–solid (m^{-1})
B - potential mass transfer index related to driving force of mass transfer (mg g^{-1})
Co - concentration of the adsorbate that enters the column (mg L^{-1})
Cs - concentration of adsorbate that leaves the column (mg L^{-1})
K_L - mass transfer coefficient (m h^{-1})
$[K_La]_d$ - porous diffusion factor or internal mass transfer factor (h^{-1})
$[K_La]_f$ - film mass transfer factor or external mass transfer factor, or volumetric film mass transfer coefficient (h^{-1})
$[K_La]g$ - global mass transfer factor (h^{-1})
q - accumulated quantity of solute adsorbed to GAC (mg g^{-1})
t - accumulation time (h)
β - adsorbate–adsorbent affinity parameter (g h mg^{-1})

2. MATHEMATICAL REPRODUCTION

The mechanism of solute adsorption on porous materials from aqueous solutions consists of the following three successive steps. First, film mass transfer or external mass transfer occurs to transport a solute from the bulk liquid to the exterior of the film zone of the grain, where it immediately connects with the pores of the grain. Second, porous diffusion or internal mass transfer occurs, allowing the solute to diffuse from the film zone toward the acceptor sites of the solid surface. Finally, fixation or adsorption of the solutes on the acceptor sites in the solid interior surfaces of the grains occurs [14].

The Langmuir constant K_L can be related to the Gibbs free energy of adsorption [15] according to the following equation: 1n $G = RT\ K_L$. In addition, a general adsorption isotherm model was developed based on the Langmuir and Freundlich models as specific cases [16]. When n = 1 (i.e., a single type of adsorption site), the Langmuir equation gives $K_{ads} = 1/K_L$. However, when the value of is small compared with that K_{ads}, this equation can be simplified.

When developing continuous equations, the following assumptions are made:

1. The surface area is considered constant over time.
2. All adsorbate molecules traversing the film zone definitely adsorb on the acceptor sites on the solid surface [14].

The data obtained by monitoring the concentrations of Hg, Cd, As, DDT, and CHLs pollution at the inlet and outlet of a Column Dynamic Reactor (CDR) were used in this study to develop continuous equations. Based on the periodically monitored adsorbate concentrations at the inlet and outlet of the system [14], the development of the mass balance equation "Entrance = Departure + Adsorbed" (see Figure 1) is reasonable. These mass transfer factor models can be used to model the mass transfer zone behaviour. They were initially developed by Fulazzaky [7], and they are applicable to the adsorption of single solutes on a porous material [8]. The mass transfer factor models modified by Fulazzaky et al. [14] were applicable for assessing the competitive effects of the adsorption of multiple solutes from contaminated water on porous materials. In this study, modified mass transfer factor models [14] have been expanded and used to determine the mass transfer resistances for the adsorption of Hg, Cd, As, DDT, and CHLs from synthetic water samples on different forms of GAC.

$$\log\left(\frac{C_o}{C_s}\right) = [k_La]_g x^{e-\beta x \log(a)} * t \qquad (1)$$

where *Co* is the solute concentration that enters the column (mg L^{-1}); *Cs*, the solute concentration that leaves the column (mg L^{-1}); $[k_La]_g$, the global mass transfer factor (h^{-1}); β, the adsorbate-adsorbent affinity parameter (g h mg^{-1}); *q*, the accumulated quantity of solute adsorbed on GAC (mg g^{-1}); *t*, the accumulation time (h); k_L, the mass transfer coefficient (m h^{-1}); *a*, the surface of interfacial liquid–solid (m^{-1}); and $[k_La]_f$, the film mass transfer factor, external mass transfer factor, or volumetric film mass transfer coefficient (h^{-1}).
Using Eq. (1), the following linear expression can be obtained mathematically:

$$\log(q) = B + \frac{1}{\beta} \times \log(t) \qquad (2)$$

$$\text{where B} = \frac{\log(kL_a)_g - \log(\log)(\frac{C_o}{C_s})}{\beta} \qquad (3)$$

Here, *B* is the potential mass transfer index, and it is related to the driving force of the mass transfer ($mg\ g^{-1}$).The correlation of the external to the global mass transfer as proposed by Fulazzaky et al. [14] can be expressed as follows:

$$[k_La]_f = [k_La]_g \times e^{-\beta \times \log(q)} \qquad (4)$$

where $[k_La]_g$ is the global mass transfer factor (h^{-1}); β, the adsorbate-adsorbent affinity parameter (g h m^{-1}); and *q*, the accumulated quantity of solute adsorbed on GAC ($mg\ g^{-1}$).

By using Eq. (4), the values for $[k_La]_f$ can be computed based on the *q* values used for plotting the linear graph, as shown in Eq. (3). This calculation is possible because parameter *B* is verified on a straight line and $[k_La]_g$ values are computed based on the outflow (%) using Eq. (3). Because the porous diffusion factor recognizes the difference between the global and the film mass transfer factor [14], the

following equation can be used:

$$[k_L a]_d = [k_L a]_g - [k_L a]_f \quad (5)$$

where $[k_L a]_d$ is the porous diffusion transfer factor (h^{-1}). Eq. (5) allows us to compute the values of $[k_L a]_d$ based on the outflow (%) because the values for both $[k_L a]_g$ and $[k_L a]_f$ have been verified.

The recorded data could be beneficial for modelling because the variations of *Cs* were monitored continuously during the experimental period. However, it is impossible to determine the variations of $[k_L a]_g$ before the passing point because the *Co/Cs* ratio is infinite, as shown in Eq. (1). Monitoring *Cs* at the outlet of the column after the passing point is important for modelling. Index *B* and parameter β should both be constant and must be verified. These values are used to validate the experimental data using linear regression techniques before calculating the variations of $[k_L a]_g$. A plot (see Eq. 2) of *Log(q)* versus *Log(t)* provides a straight line with an intercept (*B)* and slope (β^{-1}). Next, Eq. (3) is used to compute the values of $[k_L a]_g$ based on the outflow (%) (or ratio of Co/Cs) because index *B* and parameter β are verified on a straight line. Many equations that take into account the porous diffusion have been developed to determine the mass transfer resistance [17]. The porous diffusion factor is the difference between the global and the film mass transfer factor [14].

3. Pilot-scale set-up and experiment

A laboratory pilot-scale experiment was set-up using different GACs and similar flow rates to monitor the flow rates and pollutant concentrations in the influent and effluent. The temperature was monitored closely at 30±2°C. To ensure that the temperature is maintained, one regulator unit and a water circulation bath are installed in the system. Table 1 shows the dimensions of the CDR.

Table I
Dimensions of CDR

Elements	Unit	Dimension
Diameter	mm	15
Height	mm	300
Weight of GAC in column	g	2
Flow rate	cm^3/h	22.4
Initial concentration	mg/L	0.2

3.1 Activated carbon selection

Different types of GACs that were locally available are selected for use as adsorbents in this study. Two grams of three types of GAC are used as the adsorbent: GAC Filtersorb 300 (bitumen analytical grade (BAG)), OLC-W 12 x 40 (coconut shell analytical grade (SAG)), and coconut shell commercial grade (SIG). Among the GAC sources used in this study, BAG and SAG were obtained from Calgon Carbon Corporation, and SIG was produced by Effigen Carbon Sdn Bhd. Table 2 shows the specifications of the selected GACs. The GACs were rinsed with deionized water and dried in ovens at 100°C for 24 h before being used in the CDRs.

4. Results and Discussion

4.1 Adsorption of Hg, Cd, As, DDT, and CHLs (five adsorbates) on SIG, SAG, and BAG (one adsorbent)

According to Figure 1, the aggressiveness of adsorption and accumulation efficiency on SIG and SAG are slightly lower than those on BAG, except for the adsorption of CHLs. The saturation point on SIG was significant compared to that on the other adsorbents. The longer period required to become saturated and the high accumulation
rates on GAC required for removing pollutants indicate the capabilities of SIG. Therefore, SIG should be considered when selecting an adsorbent for removing organic and inorganic pollution. Validation of the experimental data showed that the accumulation rates of the adsorbates were lower than those of the other adsorbents. BAG showed good adsorption and resistance for synthetic pollutants such as DDT and CHLs. Furthermore, SIG showed reasonable adsorption for organic and inorganic removal. Additional discussions are focused on linear regression analysis. Moreover, adsorption properties can be controlled by changing the channel uniformity of a porous framework [18].

Table II
GAC's Properties

Specification	FILTERSORB 300 (BAG)	OLC-AW 12X40 (SAG)	EFFIGEN (SIG)
Mesh size 30 (mm)	86	100	96.7
Surface area (m2/g)	1077	1131	1076
Pore volume (m3)	51.34	46.48	57.63
Moisture (%)	2	Max 5	2.96
Ash content (%)	7	1	2.32
Bulk density (g/cm3)	0.56	0.7	0.49
Hardness (mg/L)	78	97	98.17
Iodine Number (mg/g)	900	1050	950
pH (units)	6.5	6	8.9

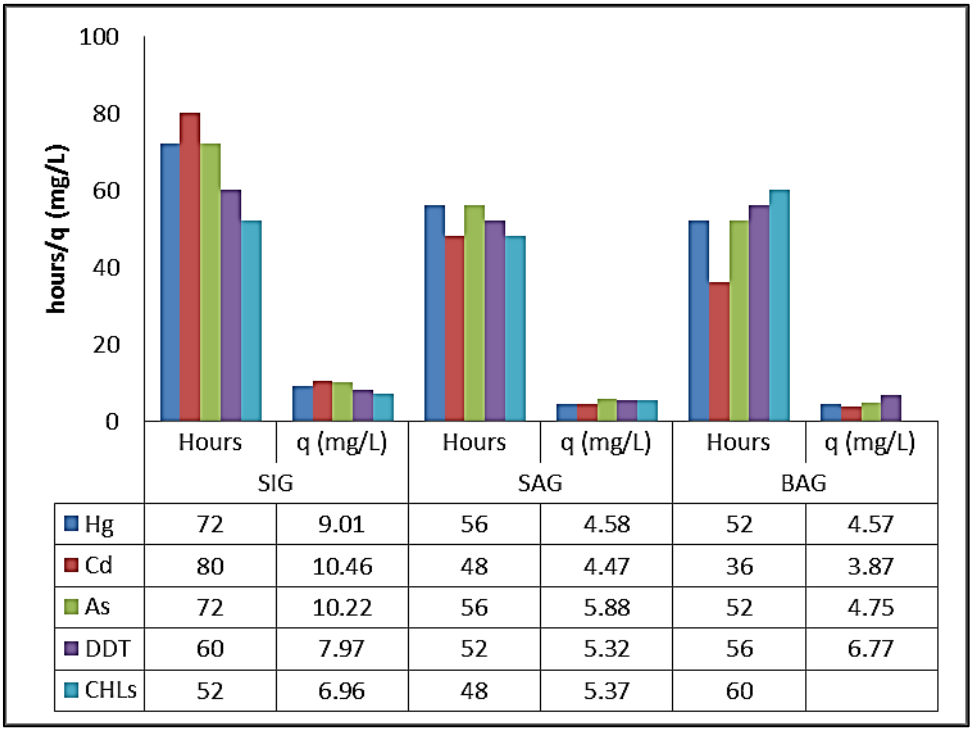

	SIG		SAG		BAG	
	Hours	q (mg/L)	Hours	q (mg/L)	Hours	q (mg/L)
Hg	72	9.01	56	4.58	52	4.57
Cd	80	10.46	48	4.47	36	3.87
As	72	10.22	56	5.88	52	4.75
DDT	60	7.97	52	5.32	56	6.77
CHLs	52	6.96	48	5.37	60	

Fig. 1. Comparison of time and accumulation rates for the various adsorbates on the different adsorbents.

An earlier study by Zabihia et al., (2009) [29], showed the adsorption isotherm of mercury ions on activated carbon on the variation of initial mercury concentration at a fixed amount of adsorbent (0.02g) per 50 mL solution was showed the adsorption isotherms for Hg sorption on walnuts carbon shell obtained for concentrations ranging from 9.7 to 107mg/L while keeping all other parameters constant. Contact time was also kept constant at 60 minutes for the equilibrium experiments. The results look not much different with the SIG adsorption on Hg. Neeta et al., (2009) [30] found that the effect of pH on the Cd adsorption characteristics of polyacrylamide grafted rice husk/sawdust was significant. Studies indicate that the system is strongly pH-dependent. The amount adsorbed is maximum at pH 9, for both adsorbents**.** Singh et al.(2006) [31] have reported maximum adsorption of cadmium at pH 8.6 in earlier studies on wheat bran. Lesser removal of metal ions at lower pH is apparently due to the higher concentration of H+ ions present in the reaction mixture that compete with the M^{2+} ions for the adsorption sites of grafted adsorbents. However, all the findings are using one pollutant onto one adsorbent. In this study, the used of five pollutants (mixed pollutants solution) is apply to investigate the mechanism of the mass transfer.

4. 2 Linear regression analysis of mixed substances adsorbed on SIG

In this study, log (*q*) was plotted versus log (*t*) (Eq. (3)) to obtain a straight line with an intercept of *B* and slope of β^{-1}. Surface adsorption and intraparticle diffusion both contributed to the actual adsorption process. The intercepts provided information regarding the thickness of the boundary layer, with larger intercepts corresponding to greater boundary layer effects. Figure 2 shows the linear regression analyses for the adsorption of Hg, Cd, As, DDT, and CHLs (mixed) on

SIG.

The significant adsorption that occurred for the mixed substance included the adsorption of CHLs (β = -2.6592 mg-1) and DDT (β = -2.7419 mg-1) on SIG. SIG was prepared at high pH (8.9 units), and it had high pore volume (57.63 m^3). The distributions of pollutants in water as a function of pH [19, 20] were indicated by the high concentrations of pollutants in water samples with pH of 3.5–4.5. The high pH in SIG (Table 2) likely played a significant role during adsorption. Acidic environments are especially interesting because the low pH of water results from the generation of H^+ ions when high levels of pollutions react with water molecules to form OH^-. It is possible that this attraction, which can result in bonding between the pollution and the alkaline functional groups, is covalent [19] and requires a long time to arrive and attach at the acceptor sites in the pores. This result is obtained because the mass transfer resistance depends on the film's mass transfer and controls the transport of pollutants from the bulk water to the film zone, which delays the diffusion of pollutants in the pores [21].

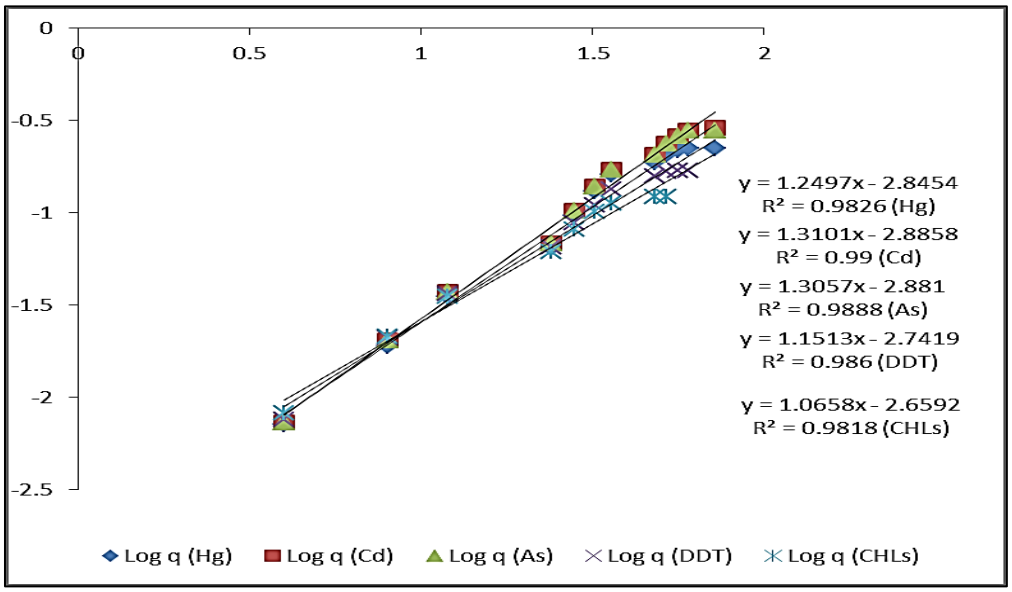

Fig. 2. Linear regression summary for adsorption of mixed solutions of Hg, Cd, As, DDT, and CHLs (five adsorbates) on SIG (one adsorbent).

High atomic weight and low density would positively impact the driving force during CHLs adsorption on SIG, followed by DDT, in which the density is lower than that of the other adsorbates and the driving force can rapidly transport organic and inorganic solutes from the bulk water to the film zone. Even when the interactions between the pollutants and the acceptor sites at the GAC surface are associated with more dominant van der Waals forces, fixation is more competitive because the pollutant concentrations in the pores are high [14].

4.3 Linear regression analysis of mixed substances adsorbed on SAG

The experimental data in Figure 3 show that the regression for the adsorption of Hg from mixed solutions on SAG is significant when the driving force for the index (β = -1.5282 mg g^{-1}) is higher than the β values for Hg, As, DDT, and CHLs. The high adsorbate-adsorbent affinity parameters for the adsorption of CHLs on SAG (1.0806 g h mg^{-1}) resulted from the activities of H^+ and Cl^- ions, which are associated in CHLs. Cl^- ions tend to associate with DDT and CHLs to bind with other adsorbates such as Cd and form $CdCl_2$; this reduced the density to 4.05 g/cm^3 and increased the molecular weight to 183.32 g mol^{-1}. The combination of these two substances produced a high driving force for Hg adsorption on SAG.

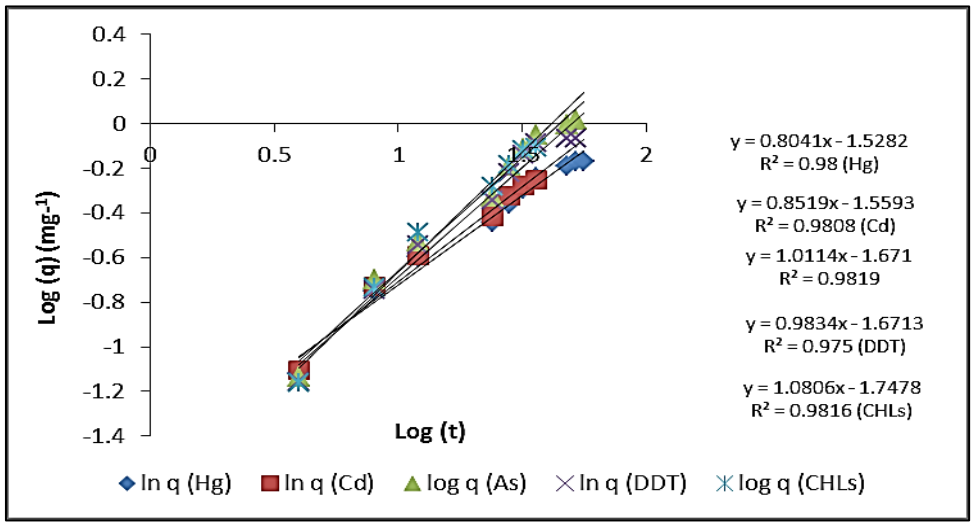

Fig. 3. Linear regression summary for adsorption of mixed solutions of Hg, Cd, As, DDT, and CHLs (five adsorbates) on SAG (one adsorbent)

The amount of iodine was the most important parameter that was used to characterize the performance of activated carbon [22]. The high amount of iodine in SAG (1050 mg/L) compared to that in SIG (950 mg/L) and BAG (900 mg/L) was significant for the adsorption of inorganic substances such as Cd and As. Furthermore, the adsorbate composition played a significant role in the adsorption process and resulted in a highly productive driving force for driving absorbance to the shell base. The atomic numbers of Hg (80), Cd (48), and As (33) need to be considered during adsorption. According to the data verification, the mesh sizes for SAG (100 mm) were slightly larger than those for BAG and SIG. The greater amount of iodine attached to SAG (1050 mg/g) played a significant role in the adsorption process on SAG. Greater amounts of iodine indicated a higher degree of GAC activation [22]. Furthermore, the affinities of the adsorbates for adsorbents such as DDT, As, and CHLs were promoted by the low density. Energetic heterogeneity is related to the properties of the adsorbate, such as the molecular structure, molecular weight, and solubility/polarity [23], and the properties of the adsorbent, such as the porosity, granulometry, and surface chemistry [24]. Micro diatom shells with high specific surface areas may be generated in a wide variety of three-dimensional shapes for tailored filtration or adsorption for water purification and solute separation [25].

4.4 Linear regression analysis of adsorption of mixed substances on BAG

Figure 4 shows a linear regression summary for the adsorption of mixed solutions on BAG. From the data shown in Figure 4, the adsorption of Hg, Cd, and As on BAG was significant. The affinities of the adsorbate-adsorbent on Hg, Cd, and As were higher during adsorption on BAG according to the β index. The smaller mesh size (86 mm) and higher ash content (7%) make BAG a good and efficient adsorbent for inorganic substances compared to organic ones. However, DDT and CHLs showed real adsorbate-adsorbent affinity and resulted in good R^2 during adsorption. Hg shows higher driving force for adsorption on BAG (-2.5945 mg g^{-1}). Theoretically, when Cl from DDT or CHLs bonds with Hg, $HgCl_2$ is formed; thus, the density of Hg decreases from 13.5336 to 5.43 g/cm^3, and its molecular weight increases from 200.59 to 271.52 g mol^{-1}. Higher ash content can hinder the adsorption of organic substances on BAG.

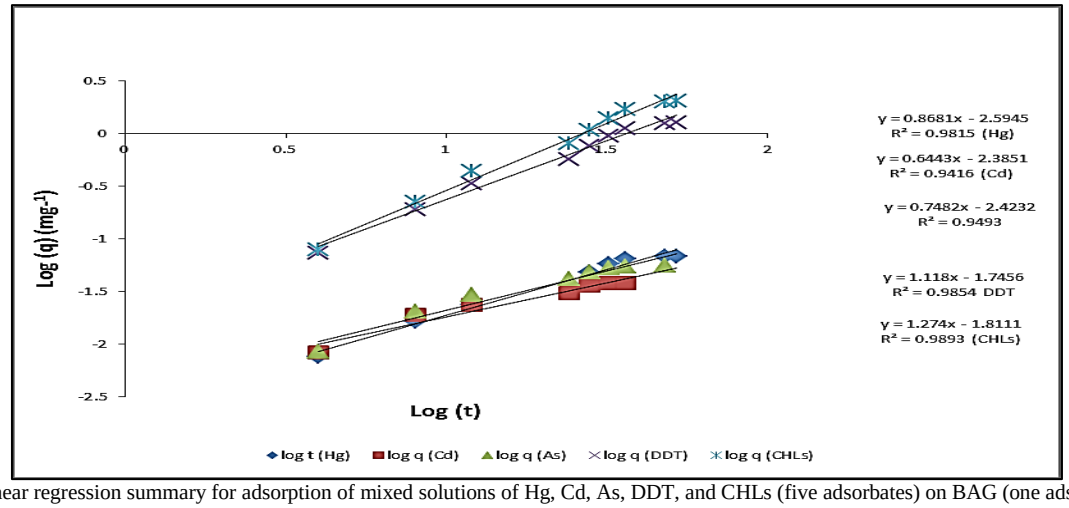

Fig. 4. Linear regression summary for adsorption of mixed solutions of Hg, Cd, As, DDT, and CHLs (five adsorbates) on BAG (one adsorbent)

The same results were obtained for As. When assuming that the Cl from DDT or CHLs bonded with As to form AsCl in the solutes, the density of As decreased from 5.73 to 2.16 g/cm^3, and the molar mass or atomic weight increased from 112.41 to 181.28 g mol^{-1}. Furthermore, the atomic weight of Hg increased from 200.59 to 236.0430 g mol^{-1} as the density decreased to 5.43 g cm^3. Therefore, the driving force decreased, and the β index values for Cd (-2.3851 mg g^{-1}) and As (-2.4232 mg g^{-1}) were lower than those for DDT and CHLs, as shown in Table 4. As indicated by the above findings, lower densities resulted in lower driving forces. These findings were verified by the data analysis. Substances with lower densities during adsorption on BAG will have lower adsorbate-adsorbent affinities, and higher atomic weights will result in a steady driving force. The potential mass transferred competition occurs when porous materials adsorb two or more adsorbates simultaneously. Physisorption occurs whenever an absorbable fluid (adsorptive) contacts the surface of the adsorbent. The properties of the adsorbents, such as porosity, granulometry, and surface chemistry, play important roles during the adsorption processes [3]. However, after breakthrough occurred, the adsorption of substances mainly occurred at acceptor sites at the outer surface of the GAC and resulted in substantial structural rearrangements [26] on the inorganic and robust sides of the interface.

5. $[k_La]_g$, $[k_La]_f$, and $[k_La]_d$ values for the adsorption of mixed substances on SIG, SAG, and BAG

Eq. 5 allows us to determine the variations of $[k_La]_d$ based on the outflow (%) if the values of $[k_La]_g$ and $[k_La]_f$ are verified. Figure 6 shows a summary of the mass transfer factors based on the outflow (%) for a mixed substance. Data validation shows significance $[k_La]_d$, $[k_La]_f$, and percentage of outflow for the adsorption of CHLs on SIG.

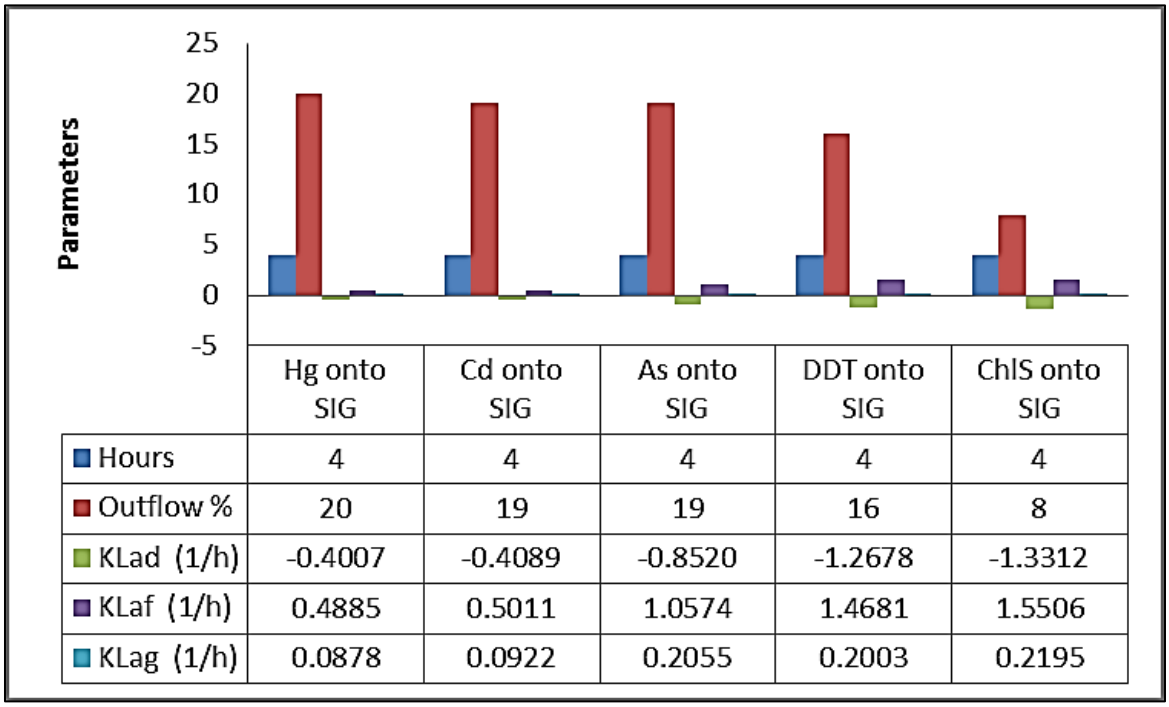

	Hg onto SIG	Cd onto SIG	As onto SIG	DDT onto SIG	ChlS onto SIG
Hours	4	4	4	4	4
Outflow %	20	19	19	16	8
KLad (1/h)	-0.4007	-0.4089	-0.8520	-1.2678	-1.3312
KLaf (1/h)	0.4885	0.5011	1.0574	1.4681	1.5506
KLag (1/h)	0.0878	0.0922	0.2055	0.2003	0.2195

Fig. 5. Summary of mass transfer factors based on outflow (%) for a mixed substance (adsorption of Hg, Cd, As, DDT, and CHL on SIG).

Figure 6 shows a summary of the mass transfer factors based on outflow (%) for a mixed substance (adsorption of Hg, Cd, As, DDT, and CHL on SAG). Hg adsorption shows good $[k_La]_d$ and $[k_La]_f$, and Cd adsorption shows good outflow (%). Figure 8 shows a summary of the mass transfer factors based on outflow (%) for a mixed substance (adsorption of Hg, Cd, As, DDT, and CHL on BAG). Cd adsorption showed significance $[k_La]_d$, $[k_La]_f$, and outflow (%).

Whenever an imbalance of solutes occurs in a medium, the solutes naturally redistribute until balance or equality is established. This tendency is often called the driving force, and it is the mechanism behind many naturally occurring transport phenomena. To balance the number of solutes per unit volume, the flow of solutes is always in the direction of decreasing concentration (from high to low concentration). The solutes gradually move away from areas of high concentration during redistribution, resulting in a diffusion process. The proportionality constant is the diffusion coefficient of the medium, which is a measure of how fast solutes diffuse in a medium. The flow is negative because the concentration decreases in the direction of flow.

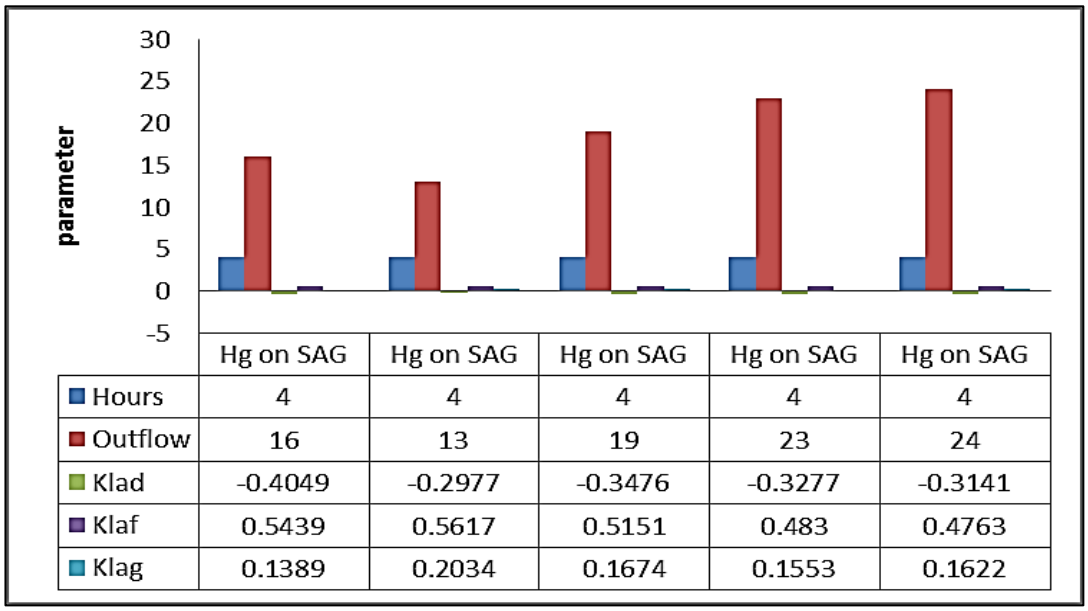

	Hg on SAG	Hg on SAG	Hg on SAG	Hg on SAG	Hg on SAG
Hours	4	4	4	4	4
Outflow	16	13	19	23	24
Klad	-0.4049	-0.2977	-0.3476	-0.3277	-0.3141
Klaf	0.5439	0.5617	0.5151	0.483	0.4763
Klag	0.1389	0.2034	0.1674	0.1553	0.1622

Fig. 6. Summary of mass transfer factors based on the outflow (%) for a mixed substance (adsorption of Hg, Cd, As, DDT, and CHLs on SAG).

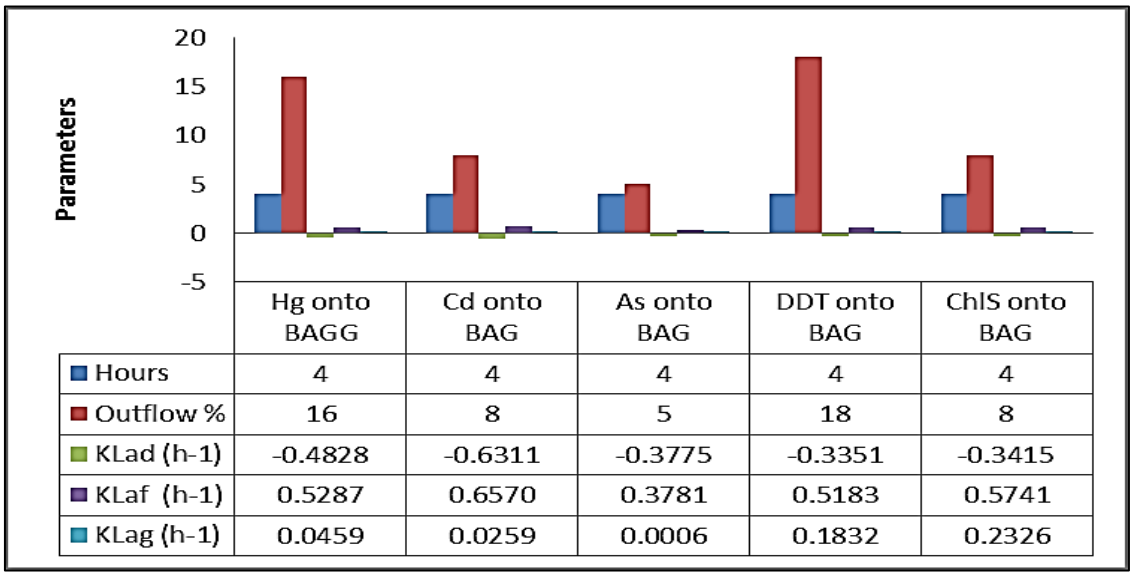

	Hg onto BAGG	Cd onto BAG	As onto BAG	DDT onto BAG	ChlS onto BAG
Hours	4	4	4	4	4
Outflow %	16	8	5	18	8
KLad (h-1)	-0.4828	-0.6311	-0.3775	-0.3351	-0.3415
KLaf (h-1)	0.5287	0.6570	0.3781	0.5183	0.5741
KLag (h-1)	0.0459	0.0259	0.0006	0.1832	0.2326

Fig. 7. Summary of mass transfer factors based on the percentage of outflow for a mixed substance (adsorption of Hg, Cd, As, DDT, and CHL on BAG)

The $[k_La]_g$ values were calculated according to Eq. (5) because the variability of the curve is crucial for assessing the global mass transfer. Thus, a plot of $[k_La]_g$ versus the outflow (%) can be proposed. The experimentally produced curve traces the variations of $[k_La]_g$ based on the outflow (%) as the cumulative variations of the curves for both $[k_La]_f$ and $[k_La]_d$, as defined by Eq. (17) (Figs. 8 (a),(b),(c), Figs. 9 (a),(b),(c), Figs.10 (a),(b),and (c). The $[k_La]_g$ curves in all of the above figures progressively transition from high to low mass transfer potential, and the $[k_La]_g$ value becomes zero when the GAC is saturated. Although decreases in the variations of $[k_La]_d$ counterbalance increases in the variation of $[k_La]_f$, the adsorption process still occurs after passing the outflow breakpoint and must consider slightly higher $[k_La]_f$ values than $[k_La]_d$ values. This result would be true even when the rate of global mass transfer decreases gradually. In this study, the speculation point is the repulsive force, which is probably in the form of a "negative $[k_La]_d$ value," and is analogous to the ionic repulsion force between the adsorbate and the acceptor sites (as if the forces from ions with the same charges that are touching each other are higher than the attractive van der Waals forces). Modified mass transfer

models have been applied to experimental data to represent breakthrough curves and determine that the mass transfer resistance depends on porous diffusion [26].

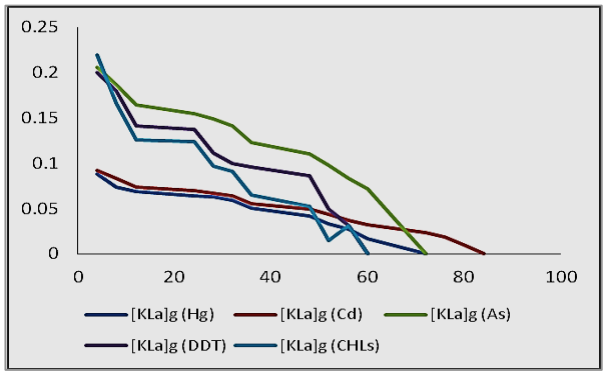

Fig. 8(a). Comparison analysis of $[K_L a]_g$ for the adsorption of Hg, Cd, As, DDT and Chlordane (mixed solutions) onto SIG pursuant to time

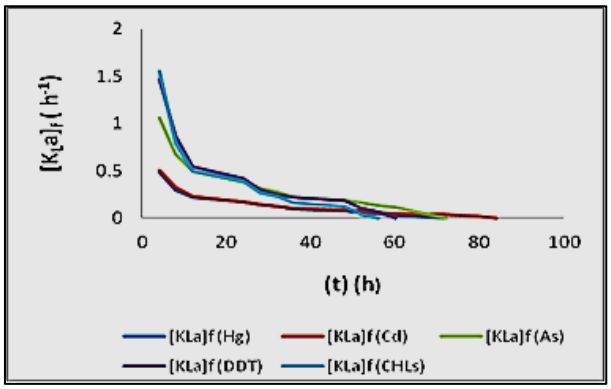

Fig. 8 (b). Comparison analysis of $[K_L a]_f$ for the adsorption of Hg, Cd, As, DDT and Chlordane (mixed solutions) onto SIG pursuant to time

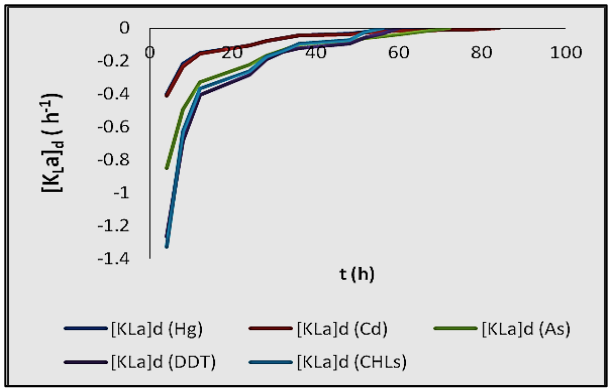

Fig. 8(c). Comparison analysis of $[K_L a]_d$ for the adsorption of Hg, Cd, As, DDT and Chlordane (mixed solutions) onto SIG pursuant to time

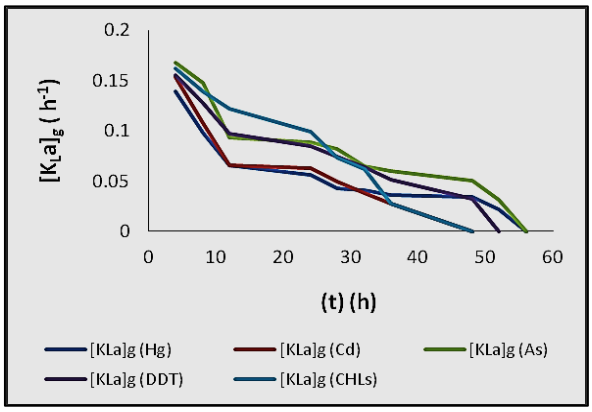

Fig. 9 (a). Comparison analysis of $[K_La]_g$ for the adsorption of Hg, Cd, As, DDT and Chlordane (mixed solutions) onto SAG pursuant to time

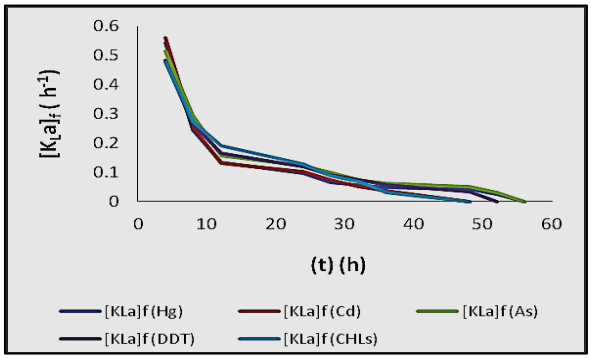

Fig. 9(b). Comparison analysis of $[K_La]g$ for the adsorption of Hg, Cd, As, DDT and Chlordane (mixed solutions) onto SAG pursuant to time

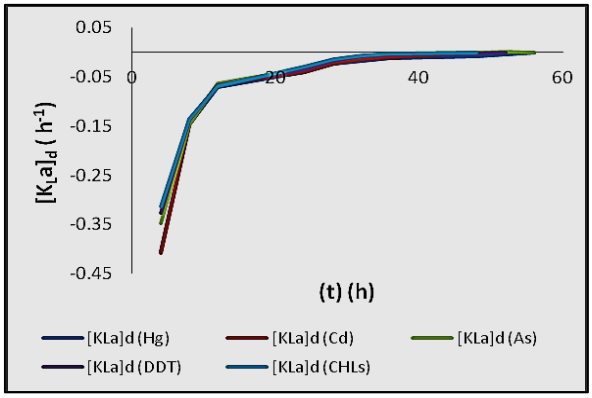

Fig. 9 (c). Comparison analysis of $[K_La]_d$ for the adsorption of Hg, Cd, As, DDT and Chlordane (mixed solutions) onto SAG pursuant to time

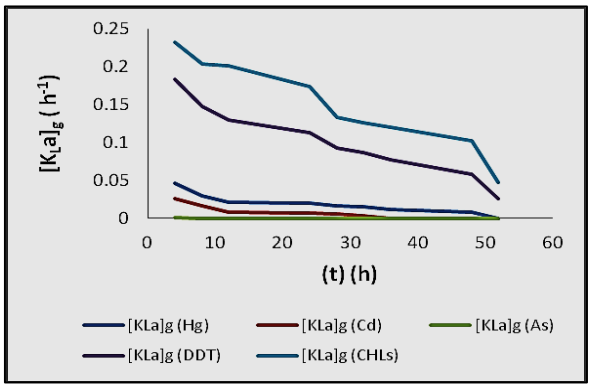

Fig. 10 (a). Comparison analysis of $[K_La]_g$ for the adsorption of Hg, Cd, As, DDT and Chlordane (mixed solutions) onto BAG pursuant to time

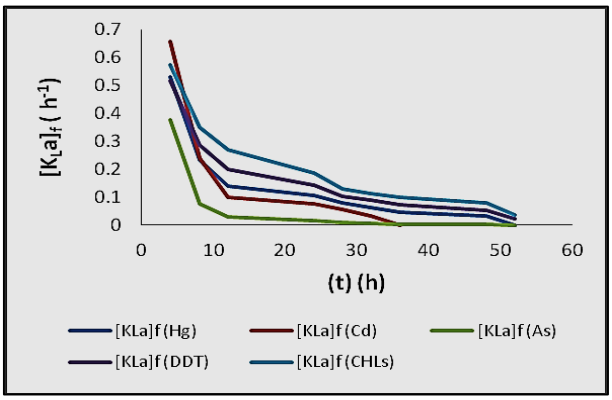

Fig. 10 (b). Comparison analysis of $[K_La]_f$ for the adsorption of Hg, Cd, As, DDT and Chlordane (mixed solutions) onto BAG pursuant to time

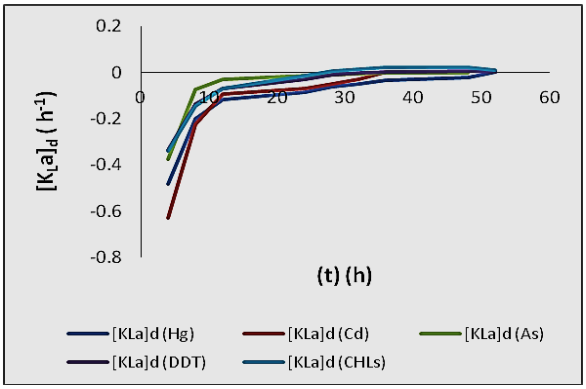

Fig. 10 (c). Comparison analysis of $[K_La]_d$ for the adsorption of Hg, Cd, As, DDT and Chlordane (mixed solutions) onto BAG pursuant to time

Choosing a GAC as a catalyst support material is critical for achieving ideal balance between the active surface sites and the solute removal performance [27]. The variations of $[k_La]_f$ and $[k_La]_d$ are both more necessary for the adsorption of substances than for the cumulative adsorption of substances when tracked separately owing to the various attractions of the substances and because the numbers of other solutes in the water sample change the k_L value. A close relationship between the chemical surface function and the global mass transfer for the GACs that originally arise from the same raw materials has been identified. This relationship suggests that the different surface chemistry potentially resulted from kinetic effects and/or ageing and involved modifications of the surface groups
[28]. The various quantities of each surface chemistry scattered to the GACs that originated from the coconut shell and bitumen potentially resulted from differences in the characteristics of the adsorbents used (Table 2).

Interspecific competition among the solutes in water samples is expected to impede solute mobility and require a long time to arrive at the outer surfaces of GAC relative to the amount of time required for it to diffuse through pores. Quick diffusion of solute molecules in pores results from the monolithic electrode of GAC with high surface area and high specific capacitance [16], and it depends on porous diffusion. This dependency occurs because it takes a long time for the diffusing solute to arrive at a deeper acceptor site compared to its movement from the bulk liquid to the film zone. The previous model can be used to predict adsorption data regardless of the concentration variations in the adsorption processes in the diffusion model in which the concentration-dependent diffusion coefficient will be used [17].

6 Conclusions

The maximum rate of porous diffusion modelled in this study was achieved when a certain outflow (%) occurred. Above this specified percentage, the curves for $[k_La]_d$ and $[k_La]_f$ are comparable, as shown in all of the above figures. Thus, the mass transfer resistance depends on the porous diffusion and film mass transfer. Because the attractive capabilities of GAC for adsorbing a substance in an aqueous solution decrease as the amount of the accumulated substance increases, the variations of $[k_La]_d$ or $[k_La]_f$ progressively decrease after passing a certain outflow (%). This result occurs because the adsorbed substances have impregnated the GAC [9]. The saturation of the GAC tested in this study was verified experimentally by monitoring the solute concentrations at the inlet and outlet of the CDR, where the GAC saturation indicated that Ce was equal to Co.

In the limiting case of infinitesimal or differential variable changes, differential equations provide precise mathematical formulations for physical principles and laws by

representing the rates of change as derivatives. Therefore, differential equations are used to investigate a wide variety of problems. However, many problems encountered in practice can be solved without resorting to differential equations or the complications associated with them. Many processes occur randomly in nature and without any specific order. These processes are governed by visible or invisible physical laws. Nonetheless, these laws consistently and predictably prevail in apparently ordinary events. Consequently, it is possible to predict the progress of an event before it occurs or to study various aspects of the event mathematically without actually running expensive or time-consuming experiments.

REFERENCES

[1] Ovez, B., Höll, W.H. (2008) adsorption of atrazine and simazine from aqueous Solutions onto poly(-caprolactone), CLEAN— Soil Air Water 36 900–904.

[2] Matsui, Y., Knappe D.R.U., Takagi R. (2002). Pesticide adsorption by granular activated carbon adsorbers: effect of natural organic matter is preloading on removal rates and model simplification, Environ. Sci. Technol. 36 3426–3431.

[3] Faur, C., Métivier-Pignon H., Pierre Le Cloirec P.(2005). Multicomponent Adsorption of pesticides onto activated carbon fibers, Adsorption 11.

[4] Ashrafizadeh, S.N., Saien J., Reza B., Nasiri M., (2008). Development of an empirical model to predict the effect of contaminants in liquid–liquid extraction, Ind.Eng. Chem. Res. 47 7242–7249.

[5] Huang, J., Yang, L., Wu, X., Xu, M., Liu, Y.N., Deng, S. (2013). Phenol adsorption on a,a dichloro-p-xylene (DCX) and 4,4 0- bis(chloromethyl)-1,1-biphenyl (BCMBP) modified XAD-4 resins from aqueous solutions, Chem. Eng. J. 222 1–8.

[6] Lytken, O., Lew, W., Campbell, C.T. (2008).Catalytic reaction energetics by single Crystal adsorption calorimetry: hydrocarbons on Pt (111), Chem. Soc. Rev. 37, 2172– 2179.

[7] Fulazzaky, M.A. (2011). Determining the resistance of mass transfer for adsorption of the surfactant onto granular activated carbons from the hydrodynamic column, Chem. Eng. J. 166 832–840.

[8] Fulazzaky, M.A. (2012). Analysis of global and sequential mass transfers for the adsorption of atrazine and simazine onto granular activated carbons from the hydrodynamic column, Anal. Methods 4 2396–2403.

[9] Davidovits, P., Kolb, C.E., Williams, L.R., Jayne, J.T. Worsnop, D.R. (2006). Mass accommodation and chemical reactions at gas– liquid interfaces, Chem. Rev. 106 1323– 1354.

[10] Holt J.K., (2006).Fast mass transport through sub-2-nanometer carbon nanotubes,Science 312 1034–1037.

[11] Scala, F. (2013). Particle-fluid mass transfer in multiparticle systems at low Reynolds Numbers, Chem. Eng. Sci. 91 90–101. P. Davidovits, C.E. Kolb, L.R.

[12] Yang K., Xing B. (2010). Adsorption of Organic compounds by carbon nanomaterials in aqueous phase: Polanyi theory and its application, Chem. Rev. 110 5989–6008.

[13] Choksi, P.M., Joshi, V.Y. (2007).Adsorption kinetic study for the removal of nickel (II) and aluminum (III) from an aqueous solution by natural adsorbents, Desalination 16– 231.

[14] Fulazzaky, M.A. (2013). Assessing the suitability of stream water for five different uses and its aquatic environment, Environ. Monit. Assess. 185 523–535.

[15] Pikaar, I., Koelmans, A.A., Van Noort, P.C.M. (2006). Sorption of organic compounds to activated carbons. Evaluation of isotherm models. Chemosphere. 65:2343-51.

[16] Liu, H., Chen, T., Chang, J., Zou, X., Frost, R.L. (2013). The effect of hydroxyl groups and surface area of hematite derived from annealing goethite for phosphate removal, J. Colloid Interface Sci. 398 88–94.

[17] Meshko, V., Markovska, L., Mincheva, M., Rodrigues, A.E. (2001). Adsorption of basic dyes on granular activated carbon and natural zeolite, Water Res. 35 3357– 3366.

[18] Matsuda, R., Tsujino, T., Sato, H., Kubota, Y., Morishige, K., Takata, M., Kitagawa,S. (2010). Temperature responsive channel uniformity impacts on highly guest-selective adsorption in a porous coordination polymer, Chem. Sci. 1 315–321.

[19] Emamjomeh, M.M., Sivakumar, M. Varyani, A.S. (2011). Analysis and the understanding of fluoride removal mechanisms by an electrocoagulation/flotation (ECF) process, Desalination 275 102–106.

[20] Widiastuti, N., Wu H., Ang H.M., Zhang D. (2011). Removal of ammonium from greywater using natural zeolite, Desalination 277 15–23.

[21] Martín, M.A., Martín, F., Kern, N. Miranda, K.R. (2010). Charge-transfer induced structural rearrangements at both sides of organic/metal interfaces, Nat. Chem. 2 374– 379.

[22] Diyuk, V. E., Zaderko, A. N., Grishchenko, L.M., Yatsymyrskiy, A. V., Lisnyak, V. V. (2012). "Efficient carbon-based acid catalysts for the propan-2-ol dehydration". Catalysis Communications 27: 33.

[23] Chatzopoulos, D., Varma A., Irvine, R.L. (2006). Adsorption and desorption studies in the aqueous phase for the toluene/activated carbon system, Environ. Prog. 13 21–25.

[24] Hollender, J., (2008). Polar Organic Micropollutants in the Water Cycle, Dangerous Pollutants (Xenobiotics) in Urban Water Cycle, pp. 103-116.

[25] Bao, Z., Song, M.K., Davis, S.C., Cai, Y., Liu, M., Sandhage, K.H. (2011). High surface Area, micro/mesoporous carbon particles with selectable 3-D biogenic dorphologies. For tailored catalysis filtration, or adsorption, Energy Environ.Sci. 4 3980–3984.

[26] Tseng, T.C., Urban, C., Wang, Y., Otero, R., Tait, S.L, Alcamí, M., Écija, D., Trelka, M., Gallego, J.M., Lin, N., Konuma, M., Starke, U., Nefedov, A., Langner, A., Wöll,C.,Herranz,

[27] Pang, W, P., Naiyun, G., Shengji, X. (2010). Removal of DDT in drinking water using nanofiltration process Desalination 250, 553–556.

[28] László, K., Rochas, C., Geissler E. (2008).Water vapour adsorption and contrast-modified SAXS in microporous polymered carbons of different surface chemistry, Adsorption 14 447–455.

[29] Zabihia, M. Ahmadpourb A., Haghighi Asla A. (2009). Removal of mercury from water by carbonaceous sorbents derived from walnut Shell. Journal of Hazardous Materials 167 (2009) 230–236

[30] Neeta, S., Kulwinder, K., Sumanjit, K. (2009). Kinetic and equilibrium studies on the removal of Cd2+ ions from water using. Journal of Hazardous Materials 163 (2009) 1338–1344.

[31] Singh, K.K., Singh,S A.K., Hasan, H. (2006). Low cost sorbent‘ wheat bran’ for the removal of cadmium from waste water:kinetic and equilibrium studies, Biores.Technol. 977 (8) 994–1001.